Analysis of bistable noise from microfabricated field emission cathodes

R. T. Olson, G. R. Condon,[a] and J. A. Panitz
Department of Physics and Astronomy, University of New Mexico, Albuquerque, New Mexico 87131

P. R. Schwoebel
Applied Physical Sciences Laboratory, SRI International, Menlo Park, California 94025

(Received 12 July 1999; accepted for publication 28 October 1999)

Field emission current fluctuations from microfabricated cathodes have been investigated. Time-correlated noise measurements and field emission electron microscope images indicate that the dominant current fluctuations are bistable in character and are emitted from a few localized sites on the cathode surface. Apertured bistable current transitions from these emission sites are often significantly larger than the percent change in total emitted current. Analysis of bistable pulse lengths has shown that the dwell time in a particular bistable emission state decays exponentially with time. Current autocorrelation measurements indicate that bistable noise at $\leqslant 300$ K is generated by adsorbates switching between emission states and not by adsorbate diffusion. © *2000 American Institute of Physics.* [S0021-8979(00)01504-8]

I. INTRODUCTION

The recent interest in vacuum microelectronics has been driven primarily by the development of low operating voltage, high current density microfabricated field electron emission cathodes.[1,2] Many possible applications of this technology are being investigated, including active elements in integrated circuits, flat-panel displays, microwave power amplifier tubes, and electron optical sources.[2–5] Short term current stability is especially important for focused electron beam optical systems because large current fluctuations at the electron source cause unacceptable variations in the beam intensity.

The field emission process is very sensitive to the conditions at the emitting surface as is evident by examining the Fowler–Nordheim equation that describes the $I-V$ characteristic of field emission cathodes,

$$J = c_1(\beta V)^2 \exp\left(-c_2 \frac{\varphi^{3/2}}{\beta V}\right), \tag{1}$$

where J is the current density, β is the electric field-voltage proportionality factor ($F=\beta V$), φ is the work function, and c_1 and c_2 are practically constants.[6,7] The exponential form of Eq. (1) illustrates that a very small change in the value of β or φ due to the presence of an adsorbate on the emitter can significantly alter the total emission current.[8–12]

Studies of thermally cleaned and annealed etched wire field emitters indicate that low frequency noise can be attributed to the surface diffusion of substrate atoms, especially at temperatures in excess of 400 K.[13] Current fluctuations occurring below the temperature required for significant adsorbate diffusion have been successfully described by a flip-flop process whereby an adsorbate switches between two different ad states corresponding to different effective work functions.[14]

Two different types of short term current fluctuations are observed to dominate the noise spectrum of single tip Spindt-type microfabricated cathodes: shot noise for frequencies >100 kHz, and ''burst'' or ''bistable'' noise at lower frequencies.[5] Bistable noise is characterized by bursts of positive or negative current pulses superimposed on a dc current level. While the bistable pulses contained within a single noise burst are similar in character, there are often dramatic differences in both magnitude and frequency between one burst and another.

This article describes investigations of the bistable current fluctuations observed from individual, microfabricated field emitter tips. Time-correlated noise measurements and field electron emission microscope (FEEM) images were used to locate active emission sites on the cathode surface. Statistical analysis of a single burst of bistable transitions allows the dwell time in a particular emission state, the magnitude of the current transition, and the underlying noise level to be determined. In addition, the bistable current autocorrelation measurements are compared to previous experimental results and the theoretical predictions made by the flip-flop mechanism for noise generation.

II. MICROFABRICATED FIELD EMITTER CHARACTERISTICS

Conventional, tungsten and molybdenum etched wire field emitters are commonly heated to ~0.8 times the melting point of the material.[7,9] This smooths the emitter surface and removes surface contaminants leaving clean, well-defined crystallographic planes exposed at the emitter apex. Further processing such as thermal field forming, field desorption, ion bombardment sputtering, and vacuum oxidation have all proven effective in changing the overall shape and emitting area.[15] Experimentally, these techniques provide a reproducible method of creating known surfaces on which adsorption/desorption, diffusion, and field emission noise measurements can be performed. Unfortunately, microfabri-

[a]Current address: Surveillance Systems, MIT Lincoln Laboratory, 244 Wood Street, Lexington, MA 02173.

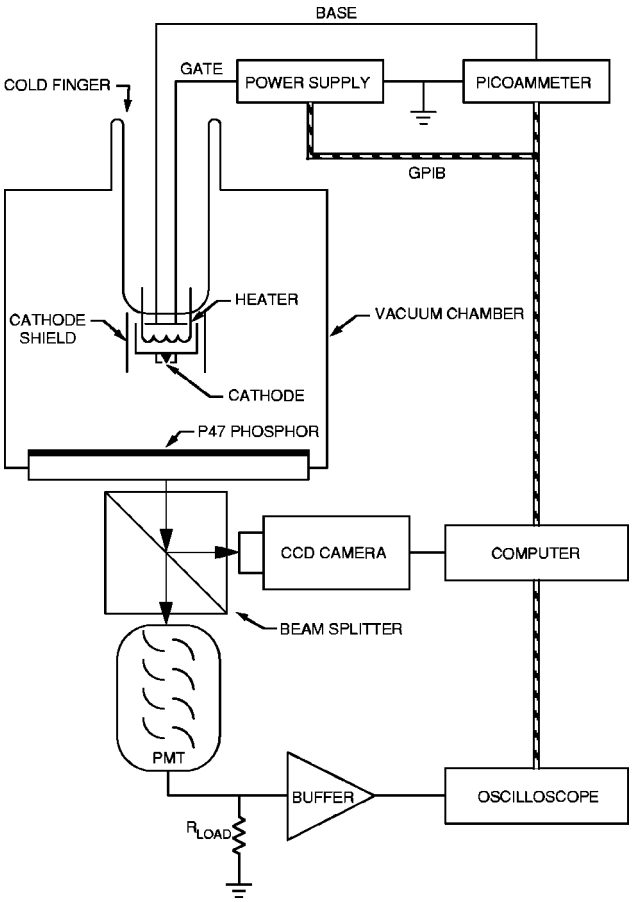

FIG. 1. Schematic of the experimental apparatus.

cated field emitters have several characteristics that can contribute to fluctuations in emission current and also inhibit the ability to understand the mechanisms that are responsible for the emission noise.

The process by which Spindt-type microfabricated field emitters are manufactured results in a highly polycrystalline, molybdenum cone that has an irregular and irreproducible emitting surface contaminated with carbonaceous material and oxides.[2,4,16] Unfortunately, the processing techniques previously mentioned for cleaning and shaping conventional field emitters cannot be effectively implemented with microfabricated cathodes.[4]

Emission area measurements indicate that the cathodes typically have very small emitting areas of 50–1000 Å^2.[2,5] Most annealed, etched wire emitters have emitting areas ~100 times greater than this value. Therefore, since field emission fluctuations have been shown to vary as $A^{-1/2}$,[17] the current noise from single microfabricated emitters tends to be much larger than is observed from conventional field emitters operating under similar conditions.

III. EXPERIMENTAL APPARATUS

The apparatus used for the experiments described here is shown schematically in Fig. 1. It consists of a stainless-steel vacuum chamber that is evacuated to less than 1×10^{-10} Torr with tandem turbomolecular pumps. A single, Spindt-type, microfabricated field emitter is mounted on a standard TO5 header that is held on a glass cold finger with six feedthrough pins. A coil of tantalum wire is placed ~5 mm behind the TO5 header and provides the ability to radiantly heat the cathode to ~1100 K. A cathodoluminescent anode consisting of a fiber-optic bundle coated with P47 phosphor was located ~7 cm from the cathode and allowed for imaging of the field emission pattern.

A beam splitter was placed in front of the fiber-optic bundle. One output of the beam splitter was monitored with a charge coupled device (CCD) camera in conjunction with a computer controlled image acquisition board (National Instruments IMAQ PCI-1408). This combination provided a method to capture and store single FEEM images in a computer at a rate of up to 30 frames per second. A Amperex 2262B photomultiplier (PMT) with a specified rise time of ~2 ns measured fluctuations in light intensity emitted from the other output of the beam splitter. A high speed, unity-gain buffer amplifier was used to drive the capacitive load of the 50 Ω coaxial cable between the photomultiplier output and a 500 MHz, Tektronix 540D digitizing oscilloscope.[18]

The mean emission current was monitored with a Keithley 486 picoammeter between the base (tip) connection of the cathode and ground. A Bertan 225-01R power supply was used to apply a positive voltage, typically 50–150 V, to the cathode gate connection. The data acquisition, processing, and analysis was performed using LabVIEW.[19]

There are several advantages to using the P47 phosphor and a PMT to measure the bistable noise fluctuations: (1) optical decoupling the noise signal reduces electrical background noise due to ground loops and electromagnetic interference, (2) the PMT provides a low noise, linear gain stage, (3) the PMT/P47 phosphor combination accurately detects very fast changes in the emission current. The maximum bandwidth of the measurement system was limited by the response of the P47 phosphor and the RC response of the PMT circuit to ≤6.4 MHz. The PMT shot noise level was less than 1% of the total emission current and allowed easy observation of bistable fluctuations that are commonly 10%–30% of the mean emission current.[20]

IV. BISTABLE EMISSION NOISE

The bistable current noise observed from microfabricated field emission cathodes is characterized by positive or negative current pulses superimposed on a dc current level as shown in Fig. 2. A sequence of bistable pulses with the same magnitude and similar pulse lengths is contained within a single burst that can last from a few milliseconds to many hours. Often two or more bursts containing bistable transitions completely different in character are superimposed in time resulting in multistable current noise. These bursts of bistable pulses often dominate the emission noise from microfabricated cathodes and this behavior has been referred to as the ''noisy mode'' of operation.[5] The noisy mode is characterized by a burst of 10 to more than 10^5 bistable transitions. Occasionally the cathode enters a more ''quiescent mode'' that can last from a few seconds to more than 10

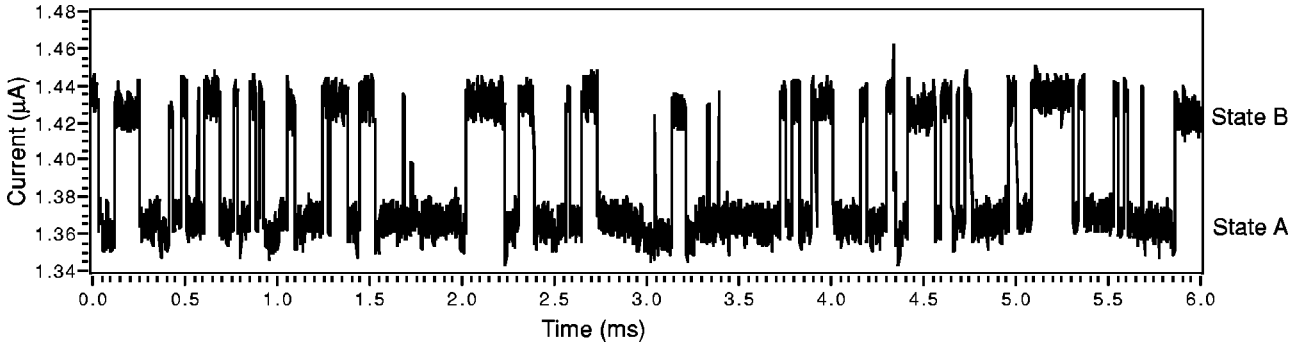

FIG. 2. One of 35 sequentially acquired bistable current waveforms when a single emission site on the cathode surface was active.

minutes when no bistable current noise is observed. The transition between a noisy and quiescent mode of operation occurs in an apparently unpredictable manner.

It was determined that the bistable transition time is <0.2 μs, but bandwidth limitations of the apparatus prevented a more precise measurement. Previous measurements of single Cs atoms switching between adsorption sites on conventional, tungsten field emitters indicate that these transitions may occur in times approaching ~ 10 ps.[21] Neither the frequency or magnitude of the bistable pulses was observed to correspond to a change in the bistable transition time.

The microfabricated cathode FEEM images are often observed to have localized emission regions that change in intensity over time. These intensity fluctuations are observed to either be randomly distributed across the emitting surface or occur from one or more fixed locations that do not change with time.[4] Large changes in both intensity and spatial distribution occasionally occur in the FEEM pattern as is shown in Fig. 3, but more often the fluctuations are characterized by only small changes in image intensity. Simultaneously, with these FEEM pattern intensity changes, the measured current is observed to fluctuate in a bistable manner.

V. TIME-CORRELATED FEEM IMAGES AND NOISE MEASUREMENTS

A. Surface localized bistable noise sources

Time-correlated bistable noise measurements and FEEM images were gathered by synchronizing the data acquisition of the oscilloscope and the IMAQ image capture board. The bistable current waveform shown in Fig. 4 contains bistable pulses with two different amplitudes. The associated time-reference waveform shown in Fig. 4 was used to select FEEM images captured before and after each bistable current transition. Subtracting the selected FEEM patterns and rescaling to enhance the contrast creates a difference image that identifies the active locations on the cathode surface corresponding to each bistable current fluctuation. It is clear from the difference images shown in Fig. 4 that the different amplitude bistable pulses were generated by changes occurring at two completely different locations on the cathode surface. If, however, a difference image is created from FEEM images acquired at the same bistable current level no significant change in the FEEM image intensity can be detected. A similar analysis can be performed for successive bistable transitions generated during a single burst as seen in Fig. 2. In this case, the same surface location is responsible for creating each of the transitions contained within the burst. It is clear from Fig. 4 that bistable current fluctuations are not necessarily associated with high emission regions on the cathode surface. Often it is difficult to observe a change in the FEEM images even though the current waveform and difference image show a bistable transition and an associated active emission site.

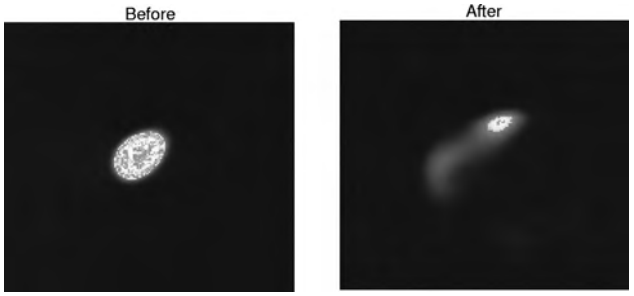

FIG. 3. FEEM images acquired before and after a bistable current transition that caused an $\sim 90\%$ change in the total emission current.

Collecting time-correlated FEEM images and noise data from a microfabricated cathode over the course of many minutes to hours has shown that at any given time there are only a few active sites (typically 3–5) generating bistable current fluctuations. These active sites are not randomly distributed across the surface of the emitter, but instead remain at a specific location on the emitter surface. Typically, each active emission site individually exhibits both noisy and quiescent behavior during an observation period.

Since only a small number of active sites exist on the emitter surface at one time and similar bistable pulses are repeatedly observed from these sites, it is reasonable to assume that the vast majority of bistable current pulses are generated by adsorbates residing on the cathode surface not by adsorption/desorption. If bistable current fluctuations were caused by either ion bombardment of the emitter surface or an adsorption/desorption event, then the active sites would appear and disappear randomly over the cathode surface. It could be argued that adsorption/desorption would preferentially occur in regions of high β due to molecular polarization effects or regions of low φ resulting in a few active sites associated with protuberances or highly chemically active sites on the cathode surface. However, this

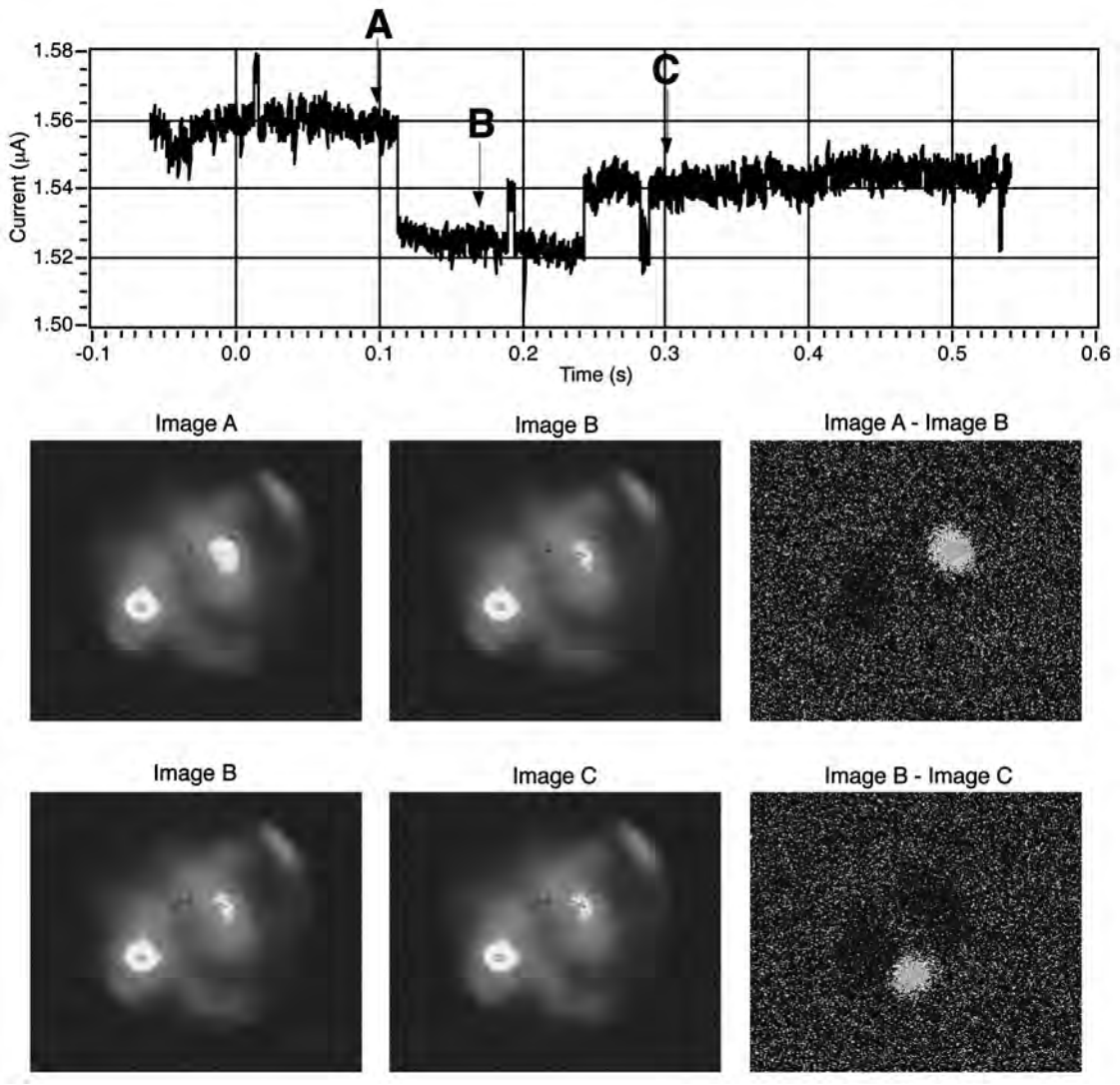

FIG. 4. Time-correlated FEEM images and bistable noise data showing the localized nature of bistable emission sites. The contrast of the difference images was enhanced by rescaling to full 8-bit resolution.

seems extremely unlikely at pressures below 1×10^{-10} Torr given that bursts of microsecond long bistable current pulses are observed from the same emission site.

B. Apertured bistable noise

Any application of microfabricated field emission cathodes (e.g., focused beam systems) that apertures the emitted current could be greatly affected if an active bistable emission site occurred within the aperture window. Time-correlated bistable noise measurements and FEEM images were used to investigate the magnitude of such changes. To accomplish this, the mean PMT output signal and total CCD luminosity were independently calibrated to the mean field emission current drawn from the cathode. Following data collection, difference images such as those shown in Fig. 4 were used to locate the active site in the associated FEEM images. A computer generated, electronic aperture was used to extract the small, active subregion from the FEEM image acquired before and after the bistable transition allowing for a measurement of the current emitted into the selected region. The validity of this measurement was independently verified by comparing the change in total current as measured by the PMT and the CCD camera for which agreement was always greater than 90%.

A typical aperture size was ~1/10 that of the total FEEM image and was sufficient to contain the entire active area as observed in the difference image. The current change in the apertured region varied widely between different active sites and, occasionally, even between different bursts of bistable pulses from a single active site. Measured changes in emission current into a apertured region are shown for a selection of bistable transitions in Table I. Choosing an aperture size smaller than the total active area indicated in the difference image decreases the measured aperture current, but the percent change in apertured current remains the same. This result suggests that at least down to the image resolution defined by the FEEM image and CCD camera, there is no discernible difference in electron emission current density within the active region.

TABLE I. Summary of measured changes in apertured emission current is shown for a selection of bistable transitions.

Active bistable sites	Total emission before	Total emission after	Total emission % change	Apertured emission before	Apertured emission after	Apertured emission % change
Site 1	0.99 μA	0.95 μA	4%	0.32 μA	0.28 μA	11%
Site 2	1.23 μA	1.19 μA	3%	0.13 μA	0.10 μA	21%
Site 3	1.58 μA	1.54 μA	3%	0.27 μA	0.24 μA	9%
Site 4	1.37 μA	1.63 μA	16%	0.69 μA	0.82 μA	20%

It is reasonable to expect differences in emitted current between active sites because there is no *a priori* reason that the same changes in β and φ would occur at different locations on the cathode surface. This is consistent with the observation that the magnitude and frequency of bistable pulses often varies widely between different active emission sites. However, it should be noted that the bistable pulses contained within the same burst resulted in similar current changes in the apertured region.

VI. BISTABLE NOISE TEMPERATURE DEPENDENCE

Microfabricated cathode temperature has been observed to significantly affect the bistable emission noise level. Although the experimental apparatus did not have the ability to accurately control the cathode temperature, the cathode could be radiatively heated to ~1100 K as determined with an optical pyrometer, and cooled to ~77 K with liquid nitrogen. In practice, bistable emission noise measurements could not be made much above room temperature because of significant ohmic leakage between the pins of the TO5 header on which the microfabricated cathodes are mounted.

Heating a microfabricated cathode with only a few active bistable sites to a temperature of ~1000 K and then cooling it to ~300 K completely changes the emission from the cathode surface. Many new active sites are observed on the surface and the current noise is characterized by a complex superposition of multiple bistable pulses. A peak-to-peak measurement of the bistable noise often shows the current fluctuations to be greater than 75% of the mean emission current. Operating the cathode for many hours, or even days, slowly decreases the noise and number of active emission sites to preheating levels. Diffusion of cathode contaminants up the side of the molybdenum cone or the transport of gas phase contaminants to the emitting surface are likely explanations for this behavior.

Cooling the microfabricated cathodes to ~77 K also has a dramatic effect on the bistable emission noise as is illustrated by Fig. 5. Both the number of active bistable emission sites and frequency of the bistable transitions are observed to decrease. However, it should be noted that although bistable current fluctuations are observed much less frequently at ~77 K, the magnitude of the transitions remains the same. This suggests that the mechanism responsible for generating a bistable noise transition is temperature dependent.

VII. BISTABLE PULSE LENGTH ANALYSIS

The observed current waveforms are most often a superposition of two or more bistable transitions generated by different emission sites on the cathode surface. Occasionally, however, a single active site will emit a burst of many bistable pulses while all other active emission sites are in a quiescent mode. The waveform shown in Fig. 2 was one of thirty five sequentially captured waveforms when this situation occurred. The current is seen to fluctuate between two distinct levels and spends a variable length of time in each emission state.

The current fluctuation histogram shown in Fig. 6 was created from the entire sequence of 35 waveforms that each captured the bistable transitions shown in Fig. 2 and were contained within the same burst. The two distinct peaks evident in the histogram correspond to the two different bistable current levels. Each peak was fit to a Gaussian distribution in order to extract information about the two emission states.

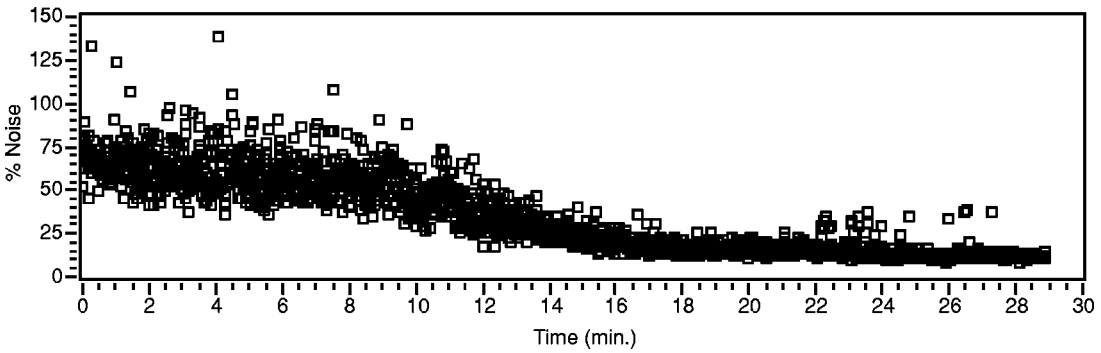

FIG. 5. Graph of percent noise vs time from a single microfabricated field emitter. The emission current noise was induced by initially heating the cathode to a temperature of ~1000 K. The cathode was cooled from ~300 to 77 K approximately 8 min after data acquisition had begun.

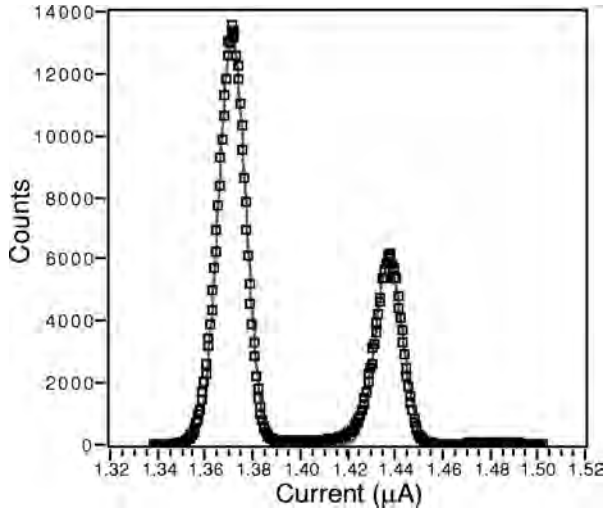

FIG. 6. Current histogram of bistable current waveforms.

The difference of the Gaussian means associated with each emission state gives the average magnitude of the bistable transition that occurred. In this case, the average bistable transition was 66 nA in magnitude. The Gaussian standard deviations provide a measure of the noise level superimposed on top of the bistable current pulses. Small values indicate the other active emission sites on the cathode surface are in a quiescent mode, while larger standard deviations result if one bistable emission site simply dominates current fluctuations generated at other locations on the cathode surface. The standard deviation for each Gaussian shown in Fig. 6 is 6 nA. Finally, a ratio of the Gaussian areas, A_A and A_B, measures the relative dwell time in each of the emission states *A* and *B*, respectively. For the data shown in Fig. 6, $A_A/A_B=2.2$ indicating that slightly more than twice the time was spent in emission state *A* than state *B*.

For a simple two-level system having discrete emission states *A* and *B*, the dwell time in each state decays exponentially with characteristic relaxation times τ_A and τ_B, respectively. Experimentally, the dwell time in each state shown in Fig. 2 was determined by measuring the lengths of time between the positive and negative going bistable transitions. A dwell time histogram for each emission state was constructed using measurements from all 35 waveforms in the acquisition sequence and is shown in Fig. 7. The relaxation times for each state were determined to be $\tau_A=96\,\mu$s and $\tau_B=36\,\mu$s from an exponential fit of the histogram data. The measurement of relative dwell times obtained from the ratio of Gaussian areas shows a 85% agreement with the ratio of relaxation times, $\tau_A/\tau_B=2.6$. Bistable dwell times ranging from a few microseconds to tens of milliseconds have been observed. It is very likely that even longer bistable dwell times occur, but have not yet been measured because other active emission sites on the cathode surface very rarely stay quiescent over long enough times to gather sufficient pulse length statistics.

The ratio of dwell times can be used to estimate the energy difference between two different emission states. Assume that the dwell time in states *A* and *B* are of the form

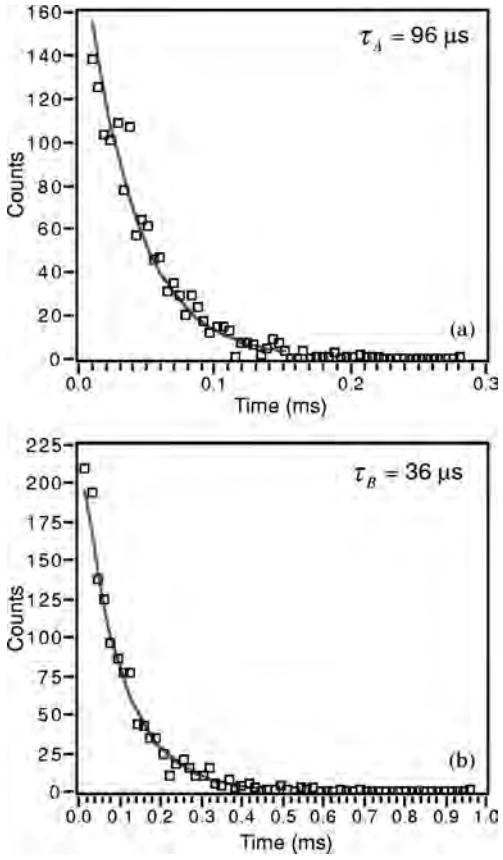

FIG. 7. (a) Histogram of dwell time measurements for the bistable emission state marked A in Fig. 4. (b) Histogram of dwell time measurements for the bistable emission state marked B in Fig. 4.

$$\tau_A^{-1}=\nu_A \exp\left(-\frac{E_{AB}}{kT}\right) \tag{2}$$

and

$$\tau_B^{-1}=\nu_B \exp\left(-\frac{E_{BA}}{kT}\right), \tag{3}$$

respectively, where ν_A and ν_B are constant frequency factors, E_{AB} and E_{BA} are the activation energies to switch from state *A* to *B* and visa versa, *k* is the Boltzmann constant, and *T* is the temperature. Solving for the energy difference, $\Delta E=(E_{BA}-E_{AB})$, between the different emission states from the ratio of τ_A and τ_B gives the equation

$$\Delta E=-kT\left[\ln\left(\frac{\tau_A}{\tau_B}\right)+\ln\left(\frac{\nu_A}{\nu_B}\right)\right]. \tag{4}$$

Given the qualitative observations that the ratio of dwell times at ~77 K is not significantly different than that observed at ~300 K it is reasonable to assume that ν_A/ν_B is small and almost certainly less than 10. Using the dwell times measured for many different bistable transitions, the energy difference at room temperature was found to range from $20\leqslant\Delta E\leqslant 200$ meV.

A previous investigation of oxygen mobility on a tungsten field emitter has been performed by Chen and Gomer.[14] The sensitivity of the field emission process to extremely small changes in β and φ makes the emitted current highly

dependent upon fluctuations in adsorbate coverage. This means that the adsorbate density autocorrelation function

$$f_n(t) = \langle \delta n(0)\, \delta n(t) \rangle, \tag{5}$$

where δn is the fluctuation in adsorbate density, is proportional to a measurement of the current fluctuation autocorrelation function, given by the equation

$$f_i(t) \cong \frac{\langle \delta i(0)\, \delta i(t) \rangle}{\overline{i}^2}, \tag{6}$$

where $\overline{i}$ is the mean emission current and δi is the magnitude of the current fluctuation.[14] The decay of $f_i(t)$ is then used to quantify fluctuations in adsorbate coverage and calculate oxygen diffusion coefficients and activation energies. Observations of small current correlation signals were also made below the diffusion temperature and were attributed to a flip-flop mechanism for oxygen atoms switching between two or more different bonding states. The following current autocorrelation function was derived by Gomer for conditions with no adsorbate diffusion

$$f_i^{AB}(t) = \overline{n}(C_A - C_B)^2 \frac{\tau_A \tau_B}{(\tau_A + \tau_B)^2} \exp\left(- \frac{t}{\tau_f} \right), \tag{7}$$

where

$$\frac{1}{\tau_f} = \frac{1}{\tau_A} + \frac{1}{\tau_B}, \tag{8}$$

$\overline{n}$ is the mean number adsorbates, and C_A and C_B are constants that account for differences in the preexponential and exponential terms in the Fowler–Nordheim equation [see Eq. (1)] when the adsorbate is in state A and state B, respectively.[22]

The process was further generalized by Chen to account for two distinct, noninteracting adsorbates on the cathode surface that are simultaneously undergoing a different flip-flop transition (i.e., $A \leftrightarrow B$ and $C \leftrightarrow D$).[14] The result is a current correlation function that is simply the sum of exponentials described by Eq. (7),

$$f_i(t) = f_i^{AB}(t) + f_i^{CD}(t). \tag{9}$$

The measurements of $f_i(t)$ shown in Fig. 8 were obtained from the microfabricated field emission cathodes by analyzing a sequence of bistable current noise waveforms. Bistable transitions with dwell times greater than a millisecond follow the behavior predicted by Eq. (9) where the sum of two decaying exponentials is responsible for the curvature in $\ln[f_i(t)]$ near $t=0$. By extrapolating the dominate exponential at long times to $t=0$ and subtracting it from $f_i(t)$ at short times, the two exponentials can be separated. However, bistable transitions with dwell times less than 100 μs more closely fit the behavior predicted by Eq. (7) as no curvature is observed in $\ln[f_i(t)]$. The difference in $f_i(t)$ for short and long dwell time bistable transitions is attributed to the increased probability that a second emission site is active during a longer duration measurement. The results shown in Fig. 8 indicate that an adsorbate flip-flop mechanism is responsible for the bistable noise generated from microfabricated field emission cathodes.

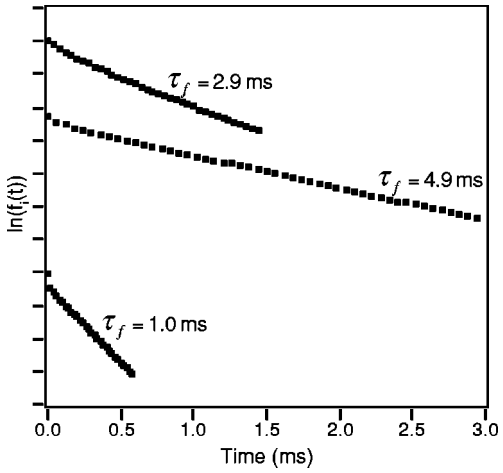

FIG. 8. Graph of $\ln[f_i(t)]$ vs time for three different waveform sequences with the measured value of τ_f for each data set shown.

VIII. CONCLUSION

The time-correlated bistable noise measurements and FEEM images have shown that bistable current fluctuations from microfabricated cathodes are generated by a few localized sites on the emitter surface. Each active site was shown to have unique emission characteristics that can change between bursts of bistable pulses. The dwell time spent in a given bistable emission state decays exponentially with time and relaxation times have been observed to range from a few microseconds to tens of milliseconds. The fact that the spatial location of the active emission sites does not change with time and that each site is observed to emit many bistable pulses indicates that most bistable emission noise transitions originate from longlived adsorbates on the cathode surface and not transient adsorption/desorption events. The decrease in bistable pulse frequency and the number of active sites observed at ~77 K is consistent with a decrease in adsorbate diffusion and flip-flop transitions. Since bistable current autocorrelation measurements show excellent agreement to the functional dependence derived by Chen and Gomer for an adsorbate flip-flop process, we conclude that the bistable noise observed from microfabricated cathodes is generated by one or more adsorbates undergoing a flip-flop mechanism on the emitter surface.

Future experiments will further quantify the nature of bistable noise from microfabricated cathodes, particularly when operating at higher pressures. Accurate control of the cathode temperature will be implemented, allowing the activation energies for adsorbate flip-flop processes to be measured. In order to determine the physical processes leading to noisy and quiescent emission modes the adsorbate species responsible should be identified, possibly by the imaging atom probe approach.[23]

ACKNOWLEDGMENTS

This project was funded by Ion Diagnostics Inc. of Santa Clara, CA. The authors would like to thank Dr. Capp Spindt of SRI International for his technical assistance and for supplying the microfabricated cathodes. The authors also ac-

knowledge many helpful discussions with Bill Parker and Alan Brodie of Ion Diagnostics Inc. and with Professor David Dunlap at the University of New Mexico.

[1] C. A. Spindt, Surf. Sci. **266**, 145 (1992).
[2] I. Brodie and C. A. Spindt, Adv. Electron. Electron Phys. **83**, 1 (1992).
[3] C. E. Holland *et al.*, IEEE Trans. Electron Devices **38**, 2368 (1991).
[4] P. R. Schwoebel and I. Brodie, J. Vac. Sci. Technol. B **13**, 1391 (1995).
[5] C. A. Spindt *et al.*, J. Appl. Phys. **47**, 5248 (1976).
[6] R. H. Fowler and L. W. Nordheim, Proc. R. Soc. London, Ser. A **119**, 173 (1928).
[7] W. P. Dyke and W. W. Dolan, Adv. Electron. Electron Phys. **8**, 89 (1956).
[8] C. B. Duke and M. E. Alferieff, J. Chem. Phys. **46**, 923 (1967).
[9] R. Gomer, *Field Emission and Field Ionization* (American Institute of Physics, New York, 1993).
[10] R. Gomer, Surf. Sci. **299/300**, 129 (1994).
[11] D. J. Rose, J. Appl. Phys. **27**, 215 (1956).
[12] I. Giaever, Surf. Sci. **29**, 1 (1972).
[13] L. W. Swanson, Surf. Sci. **70**, 165 (1978).
[14] J. R. Chen and R. Gomer, Surf. Sci. **79**, 413 (1979).
[15] E. W. Müller, Ergeb. Exakten. Naturwiss. **27**, 290 (1953).
[16] I. Brodie, Surf. Sci. **70**, 186 (1978).
[17] H. D. Beckley, *Field Ionization Mass Spectroscopy* (Pergamon, New York, 1969).
[18] National Semiconductor, Part No. LH0063 Ultra Fast Buffer.
[19] National Instruments, LabVIEW Software, Austin, TX 78759-3504.
[20] Philips Photonics, *Photomultiplier Tubes: Principles and Applications* (Philips Photonics, Brive, France, 1994).
[21] H. Heinzelmann, F. Watanabe, and G. McClelland, Phys. Rev. Lett. **70**, 3611 (1993).
[22] R. Gomer, Surf. Sci. **39**, 373 (1973).
[23] J. A. Panitz, Prog. Surf. Sci. **8**, 219 (1978).